THE JOURNAL OF PHYSICAL CHEMISTRY B

Article

pubs.acs.org/JPCB

The Hydrogen-Bonded Dianion of Vitamin K_1 Produced in Aqueous–Organic Solutions Exists in Equilibrium with Its Hydrogen-Bonded Semiquinone Anion Radical

Zhen Hui Lim, Elaine Lay Khim Chng, Yanlan Hui, and Richard D. Webster*

Division of Chemistry and Biological Chemistry, School of Physical and Mathematical Sciences, Nanyang Technological University, Singapore 637371

Supporting Information

ABSTRACT: When the quinone, vitamin K_1 (VK_1), is electrochemically reduced in aqueous-acetonitrile solutions (CH_3CN with 7.22 M H_2O), it undergoes a two-electron reduction to form the dianion that is hydrogen-bonded with water $[VK_1(H_2O)_y^{2-}]$. EPR and voltammetry experiments have shown that the persistent existence of the semiquinone anion radical (also hydrogen-bonded with water) $[VK_1(H_2O)_x^{-\bullet}]$ in aqueous or organic–aqueous solutions is a result of $VK_1(H_2O)_y^{2-}$ undergoing a net homogeneous electron transfer reaction (comproportionation) with VK_1, and not via direct one-electron reduction of VK_1. When 1 mM solutions of VK_1 were electrochemically reduced by two electrons in aqueous-acetonitrile solutions, quantitative EPR experiments indicated that the amount of $VK_1(H_2O)_x^{-\bullet}$ produced was up to approximately 35% of all the reduced species. *In situ* electrochemical ATR-FTIR experiments on sequentially one- and two-electron bulk reduced solutions of VK_1 (showing strong absorbances at 1664, 1598, and 1298 cm^{-1}) in CH_3CN containing <0.05 M H_2O led to the detection of $VK_1^{-\bullet}$ with strong absorbances at 1710, 1703, 1593, 1559, 1492, and 1466 cm^{-1} and $VK_1(H_2O)_y^{2-}$ with strong absorbances at 1372 and 1342 cm^{-1}.

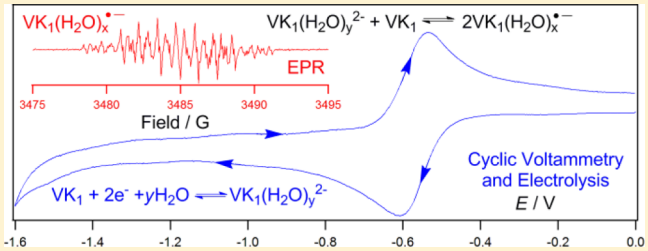

1. INTRODUCTION

Vitamin K_1 (VK_1) (phylloquinone) is a lipophilic compound based on the 2-methyl-1,4-naphthoquinone derivative with an additional phytyl side chain at the R position in Scheme 1. VK_1 is commonly found in green leafy vegetables, but it is not readily bioavailable due to tight binding to the thylakoid membranes in the chloroplasts.[1] Therefore, a significant portion of the intake of VK_1 required for human health is instead produced by the bacteria living within the colon.[2] VK_1 has several known biological roles which include functioning as electron carriers in oxidative phosphorylation during cellular respiration and as cofactors in blood clotting processes.[3,4] These roles mainly involve VK_1 taking part in a redox mechanism within the hydrophobic cell membranes; therefore, there is a motivation to understand its electrochemical properties in low-water environments such as aprotic organic solvents.

Scheme 1. Electrochemical Reduction of Vitamin K_1 in Dry CH_3CN

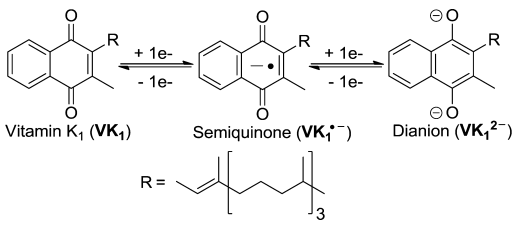

Electrochemical studies have shown that VK_1 undergoes two chemically reversible one-electron reduction processes in aprotic organic solvents under low-water conditions (Scheme 1),[5,6] similar to what is observed for most quinones (Figure 1, dotted red line).[7] In CH_3CN (containing 0.2 M Bu_4NPF_6 and 0.05 M H_2O), VK_1 is first reduced at approximately −1.2 V vs

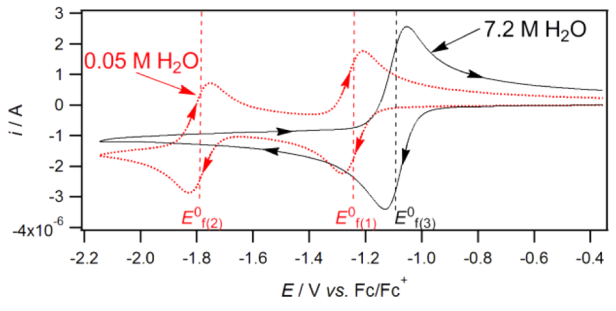

Figure 1. CVs of 1×10^{-3} M VK_1 in CH_3CN (containing 0.2 M Bu_4NPF_6 and varying water concentrations) at 293 K with a 1 mM diameter GC disk working electrode at a scan rate of 0.1 V s^{-1}.

Received: January 13, 2013
Revised: February 11, 2013
Published: February 11, 2013

Fc/Fc^+ to form the radical anion ($VK_1^{-\bullet}$) (eq 1), which is further reduced at approximately −1.8 V vs Fc/Fc^+ to form the dianion (VK_1^{2-}) (eq 2).[5]

$$VK_1 + e^- \rightleftharpoons VK_1^{-\bullet} \qquad E^0_{f(1)}/V \qquad (1)$$

$$VK_1^{-\bullet} + e^- \rightleftharpoons VK_1^{2-} \qquad E^0_{f(2)}/V \qquad (2)$$

$$VK_1 + 2e^- + yH_2O \rightleftharpoons VK_1(H_2O)_y^{2-} \qquad E^0_{f(3)}/V \qquad (3)$$

$$VK_1 + 2e^- + 2H^+ \rightleftharpoons VK_1H_2 \qquad E^0_{f(4)}/V \qquad (4)$$

The formal reduction potentials of quinones (E^0_f) in organic solvents are difficult to define exactly because they are highly dependent on the water content of the solvent.[5,6] Studies have shown that, as the water content increases, both reduction processes shift to more positive potentials with no loss of chemical reversibility, and this effect is associated with strong hydrogen bonding between water and the reduced species of VK_1.[5,6,8] It has also been observed that $E^0_{f(2)}$ shifts much more positively than $E^0_{f(1)}$ when water is added, which results in the two one-electron processes eventually merging into a single two-electron reduction step (Figure 1, black line), according to eq 3.[5] Similarly, in unbuffered aqueous solutions with pH ≥ 7, the reduction of quinones occurs in one two-electron step to form the hydrogen-bonded dianion (eq 3), while in buffered aqueous solutions at low pH the reduction occurs *via* two electrons and two protons to form the hydroquinone (eq 4).[9] Nevertheless, although the reactions in eqs 3 and 4 occur in one observable voltammetric process, the individual electron transfer steps may occur sequentially if the potentials are very closely spaced (within ∼30 mV), or if the second electron transfer occurs at a lower potential than the first transfer.[10] Therefore, in the presence of large amounts of water (and the absence of acid), VK_1 should always be directly reduced to the hydrogen-bonded dianion [$VK_1(H_2O)_y^{2-}$]. The number of water molecules (y in eq 3) involved in the hydrogen bonding is likely to vary depending on the bulk concentration of water and properties of the organic solvent.

Despite the voltammetric reduction of VK_1 in the presence of water being known to occur in one two-electron process to form $VK_1(H_2O)_y^{2-}$,[5,6] there are reports of the radical anion (likely to be the hydrogen-bonded form, $VK_1(H_2O)_x^{-\bullet}$), being detected in purely aqueous media when studied by EPR spectroscopy.[11] The probable explanation for the existence of $VK_1(H_2O)_x^{-\bullet}$ is an equilibrium comproportionation reaction involving the dianion and starting material (eq 5).[5,8] It is also possible that the reaction occurs through an intermediate dimer dianion (eq 6), which dissociates into the two anion radicals, rather than *via* the direct electron transfer of eq 5.[5]

$$VK_1^{2-} + VK_1 \rightleftharpoons VK_1^{-\bullet} + VK_1^{-\bullet} \qquad (5)$$

$$VK_1^{2-} + VK_1 \rightleftharpoons (VK_1)_2^{2-} \qquad (6)$$

There are several electrochemical studies that have reported that the dianions of quinones (Q^{2-}) undergo comproportionation reactions with their neutral starting materials (Q) to form the anion radicals ($Q^{-\bullet}$), including anthraquinone and benzoquinone in organic solvents[12−14] and benzoquinone in unbuffered aqueous solutions.[14,15] In buffered solutions with pH 7.4, quinone anion radicals have been observed by EPR spectroscopy due to a comproportionation reaction involving the hydroquinone (QH_2) and Q starting material (eq 7).[16]

$$QH_2 + Q \rightleftharpoons 2Q^{-\bullet} + 2H^+ \qquad \text{Buffered pH} = 7.4 \qquad (7)$$

Voltammetry experiments have demonstrated that, in the presence of even trace amounts of water, quinones and especially their reduced forms always undergo some degree of hydrogen-bonding interactions.[5,6] Therefore, the species present in eqs 5−7 should ideally be represented as hydrogen-bonded with variable numbers of water molecules. In this work, the formation of $VK_1(H_2O)_x^{-\bullet}$ in CH_3CN under high-water conditions has been investigated using electrolysis/coulometry combined with EPR spectroscopy. By comparing EPR signal intensities in "dry" and wet conditions, it was possible to determine the absolute amounts of semiquinone radicals produced from their dianions due to the homogeneous electron transfer reaction (eq 5). The radical anion and dianion were also investigated by *in situ* ATR-FTIR spectroscopy during electrolysis experiments in "dry" CH_3CN.

2. EXPERIMENTAL SECTION

2.1. Chemicals. VK_1 (Merck KGaA) and AR grade CH_3CN (RCI Labscan) were used as received. Ultrapure H_2O with resistivity ≥18 MΩ cm was obtained from a water purification system (ELGA Purelab Option-Q). Bu_4NPF_6 was prepared by reacting equivalent molar amounts of Bu_4NOH (Alfa Aesar) and HPF_6 (Fluka), washing the resultant precipitate with hot H_2O, and recrystallizing from hot AR grade EtOH (Merck KGaA). Purified Bu_4NPF_6 crystals were dried under a vacuum at 140 °C for 6 h and stored in a desiccator under vacuum conditions.

2.2. Cyclic Voltammetry (CV) and Controlled Potential Electrolysis (CPE). CV and CPE experiments were conducted at 22 ± 2 °C using a computer controlled potentiostat (Eco Chemie BV Autolab) in conjunction with a 1 mm diameter glassy carbon (GC) disk working electrode (for CV), a 1 mm diameter by 10 cm length GC rod working electrode (for electrolysis), an Ag wire reference electrode (connected to the analyte solution via a salt bridge containing 0.5 M Bu_4NPF_6 in CH_3CN), and a Pt mesh auxiliary electrode.

CPE experiments were conducted at specific controlled potentials depending on the water content of the solutions and were stopped when a predetermined amount of charge (Q, C) was passed. The charge was related to the average number of electrons transferred per molecule (n), the number of moles of starting material (N), and the Faraday constant (96 485 C mol^{-1}) according to eq 8. The electrolysis reactions were stopped when the calculated Q values matched the required n values. Non-whole-number n values indicate that the reaction was allowed to progress to partial completion. The potential for electrolysis was set 0.2 V more negative than the first one-electron reduction step for low-water conditions (eq 1) or 0.2 V more negative than the two-electron reduction step (eq 3) for high-water conditions.

$$Q = nNF \qquad (8)$$

2.3. Electron Paramagnetic Resonance Spectroscopy. CH_3CN/Bu_4NPF_6 solutions containing the electrogenerated radicals were quantitatively analyzed at 22 ± 2 °C in a silica flat cell with an EPR spectrometer (Bruker Biospin ELEXSYS-II E500) using two modulation amplitudes. Where interest was in obtaining the optimal EPR spectrum for structure analysis, the modulation amplitude was 0.05 G. In situations where interest was in comparing the signal intensity between experiments, the modulation amplitude was 10 G. In both cases, the sweep time

dx.doi.org/10.1021/jp4003966 | J. Phys. Chem. B 2013, 117, 2396−2402

was 30.72 s, the time constant was 1.28 ms, and the microwave power was 0.2 mW (corresponding to attenuation = 25 dB, which was sufficiently high to avoid sample power saturation).

2.4. Karl Fischer Coulometric Titrations. The water content of VK_1 solutions was measured using a Karl Fischer (KF) coulometer (Mettler Toledo DL32)—with HYDRANAL-coulomat CG (Riedel-deHaën) for the cathode compartment and HYDRANAL-coulomat AG (Riedel-deHaën) for the anode compartment—within a sealed chamber (Coy Laboratory Products) controlled at 30% relative humidity.

2.5. EPR Experiments in Low-Water Conditions. VK_1 was electrolyzed in the two-compartment electrolysis cell (section 2.2). The working electrode compartment contained 1 mM VK_1 in CH_3CN with 0.2 M Bu_4NPF_6, and the auxiliary electrolyte compartment contained 0.2 M Bu_4NPF_6 in CH_3CN. A 1 mL portion of the VK_1 solution was first taken to measure its water content (section 2.4). CV measurements with a 1 mm diameter planar GC electrode were performed under an argon atmosphere after deoxygenating the remaining solution to obtain an appropriate potential for the electrolysis. The electrolysis was conducted with the GC rod electrode under a stream of argon bubbles to stir the solution and maintain oxygen-free conditions.

After electrolysis was halted (designated as T = 0 min), a portion of the resultant electrolyzed solution was transferred into an EPR flat cell that was kept under a nitrogen atmosphere in a Schlenk type flask. At T = 15 min, EPR measurements were conducted using the parameters listed in section 2.3, and more readings were taken at T = 25, 35, and 45 min. Experiments were repeated for n = 0.2, 0.4, 0.6, 0.8, and 1.0 electrons per molecule and in duplicate for each n value with the silica flat cell placed in the same position in the EPR cavity.

2.6. EPR Experiments in High-Water Conditions. Working electrode compartment solutions (1 mM VK_1 in CH_3CN containing 0.2 M Bu_4NPF_6 and 7.22 M H_2O) and auxiliary electrode compartment solutions (0.2 M Bu_4NPF_6 in CH_3CN containing 7.22 M H_2O) were prepared as described in section 2.5 except KF coulometric titrations were not conducted because of the known amount of water added to the VK_1 solutions. The added water was in sufficiently large amount that the original water content of CH_3CN became negligible. The electrolysis was stopped when the amount of charge passed corresponded to n = 0.2, 0.4, 0.6, 0.8, and 1.0 electrons per molecule; experiments at each n value were performed in duplicate.

2.7. ATR-FTIR Experiments. Solution-phase background subtracted *in situ* FTIR experiments were conducted with a Mettler Toledo iC10 spectrometer utilizing a diamond composite ATR fiber conduit probe inside the working electrode compartment of a controlled potential electrolysis cell.[17]

3. RESULTS AND DISCUSSION

3.1. Trends in Cyclic Voltammetric Measurements. Figure 2a shows the CVs of VK_1 obtained in the electrolysis cell under low- and high-water conditions. KF titrations indicated that, in the low-water-content conditions, the initial water concentration in the electrolysis cell varied between 0.009 and 0.025 M at the start of the electrolysis. At the completion of the electrolysis, the water content was measured to be approximately 0.05 M, with the increase in water expected due to the high humidity of the local environment and the difficulty in keeping electrochemical cells completely sealed to the atmosphere.[18] Figure 2a demonstrates that VK_1 undergoes two one-electron reduction processes in CH_3CN with low water content, while VK_1 undergoes one two-electron reduction process in CH_3CN with high water content (7.22 M H_2O) in the CPE cell. Because the voltammetric potential was measured against the Ag wire reference electrode, the potentials depicted in Figure 2a are expectedly different from those depicted in Figure 1 where the potentials were measured against ferrocene.

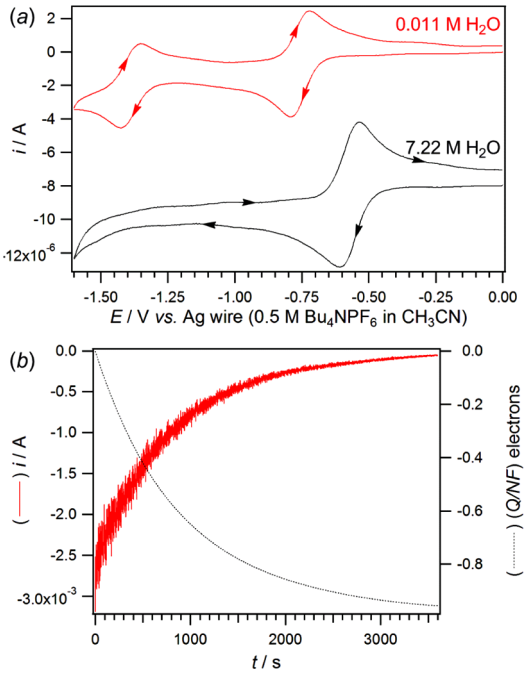

Figure 2. (a) CVs of 1 × 10^{-3} M VK_1 in a CPE cell in CH_3CN containing 0.2 M Bu_4NPF_6 at 293 K with a 1 mM diameter GC disk working electrode at a scan rate of 0.1 V s^{-1} in the presence of 0.011 and 7.22 M H_2O. (b) Current/coulometry vs time data obtained during the exhaustive reduction of 1 × 10^{-3} M VK_1 at −0.9 V vs Ag wire in CH_3CN containing 0.2 M Bu_4NPF_6 and between 0.011 and 0.05 M H_2O.

3.2. EPR Spectroscopy. Representative first derivative EPR spectra obtained from the electrolyzed solutions at different water concentrations (0.05 and 7.22 M) are provided in Figure 3a and b for modulation amplitudes of 0.05 and 10 G, respectively. The overmodulated spectra shown in Figure 3b were obtained in order to compare signal intensities (after integration) between electrolysis experiments performed with different amounts of charge passed. Since the EPR experiments were performed using identical instrumental parameters and with the sample placed in the same position within the EPR cavity, it was possible to directly compare the signal intensities across the different experiments.

The spectrum shown in Figure 3a that was obtained at low modulation amplitude and low water content is similar to what has previously been observed and assigned to the VK_1 radical anion in organic solvents.[19−23] The total widths of the EPR spectra obtained in low- and high-water-content solutions were the same, although the shapes of the spectra were different, indicating slightly different hyperfine coupling constants. It is known that semiquinone anion radicals undergo hydrogen bonding in pure water (or in alcohols), with the interactions having been detected by Q-band pulse ^2H electron−nuclear double resonance experiments.[24] It is also known from CV

dx.doi.org/10.1021/jp4003966 | J. Phys. Chem. B 2013, 117, 2396−2402

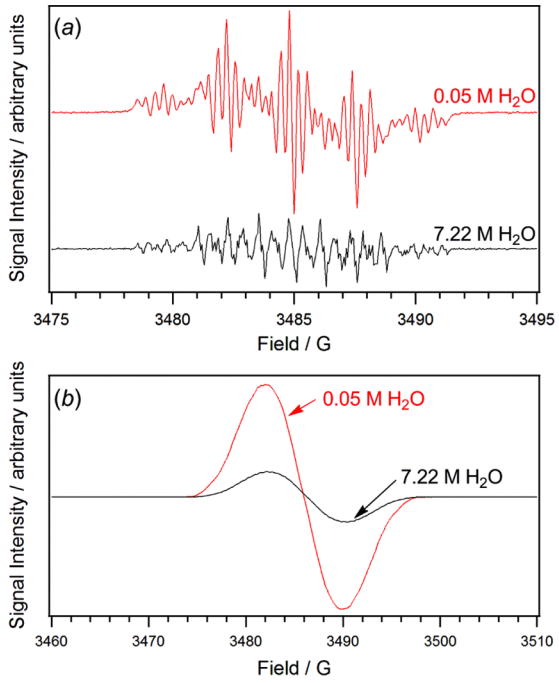

Figure 3. EPR spectra obtained of electrolyzed solutions of 1×10^{-3} VK_1 (n = 0.4 electrons per molecule) in CH_3CN containing 0.2 M Bu_4NPF_6 in a silica flat cell at 22 ± 2 °C with 0.05 and 7.22 M H_2O, obtained 15 min after completion of electrolysis: (a) modulation amplitude = 0.05 G; (b) modulation amplitude = 10 G.

measurements that $VK_1^{-\bullet}$ undergoes weak hydrogen-bonding with low concentrations of water while VK_1^{2-} undergoes much stronger interactions with even trace water.[5] Therefore, the difference between the two spectra in Figure 3a is likely due to $VK_1^{-\bullet}$ existing largely in a non-hydrogen-bonded form at low concentrations of water (<0.05 M) and in a hydrogen-bonded form $[VK_1(H_2O)_x^{-\bullet}]$ at high water concentrations (7.22 M).

The lifetime of the radical in the presence of different concentrations of water and at varying amounts of electrolysis was measured by comparing the peak signal intensity of the overmodulated spectra at different times after the completion of the electrolysis. Figure 2b shows a typical current/coulometry vs time trace for the electrolysis of VK_1, which took approximately 1 h to conclude exhaustively. Electrolysis reactions that were stopped before total completion took less than 1 h; therefore, to standardize all experiments, the electrolyzed solution was left in the cell for a total of 60 min after first commencing the electrolysis. The electrolysis reaction was performed at a GC rod working electrode rather than a platinum electrode to avoid the likelihood of electrolyzing water in the high-water-content solutions (since the reduction of H_2O is more kinetically favored on Pt compared to GC). Calibration experiments performed by electrolyzing solutions containing 7.22 M H_2O (but no VK_1) at the GC rod electrode at the same potential used for the VK_1 solutions indicated that the contributions of the background electrolysis currents were negligible (<1%) to the overall charge for VK_1 reduction.

Tables S1 and S2 in the Supporting Information give the relative peak signal intensities of the EPR spectra at t = 15, 25, 35, and 45 min after electrolysis under low-water and high-water conditions, respectively. In each case, the same instrumental conditions were used; therefore, the absolute peak intensities provide a good estimate of the amount of radicals that are present relative to each experiment.

The experiments were repeated in duplicate for each electrolysis level (0.2−1.0 electrons per molecule), and in most cases, there was only a small difference between them. It was found that the EPR peak signal intensities decreased by a relatively small amount over 30 min (<10%), indicating that $VK_1^{-\bullet}$ is long-lived in the CH_3CN solutions. It was also noted that the peak signal intensities under high-water conditions decreased slower over time as compared to low-water conditions. The reason for this could be due to the lower reduction potential of the hydrogen-bonded species in the high-water-content solutions, which are less likely to undergo electron-transfer reactions with trace impurities.

A feature that is apparent by comparing the spectra in Figure 3b (and Tables S1 and S2 in the Supporting Information) is that the EPR signal intensities of $VK_1(H_2O)_x^{-\bullet}$ produced in the high-water-content environment (7.22 M) are substantially less than the signals in the low-water-content (0.05 M) environment, for equivalent n values. The decrease in signal intensity is not due to differences in reactivity, since the longer time scale experiments indicate that the radical decays relatively slowly, and the radicals in the high-water-content solution appear even longer lived than in the drier solvent. In the low-water-content experiments, the applied potential for the electrolysis is only sufficiently negative to produce $VK_1^{-\bullet}$ (and not VK_1^{2-}), but for the high-water-content solutions, the same applied potential will immediately produce VK_1^{2-}. Therefore, the most likely explanation for the detection of radicals in the high-water-content environment is via the comproportionation mechanism in eq 5.

In order to obtain a more accurate comparison of the signals, each of the overmodulated spectra at t = 15 min was integrated (the area under the graphs is representative of the total concentration of $VK_1^{-\bullet}$) and the average values taken from the duplicate measurements at each n value. The EPR signal intensity values in the low-water-content solutions at n = 0.2, 0.4, 0.6, 0.8, and 1.0 electrons per molecule conversion (corresponding to 0.2, 0.4, 0.6, 0.8, and 1.0×10^{-3} M $VK_1^{-\bullet}$) were scaled to 0.20, 0.40, 0.60, 0.80, and 1.00×10^{-3} M, respectively (assuming no decomposition occurred during the time scale of the experiment). The intensities of the EPR signals obtained in the high-water-content solutions were normalized with respect to their low-water-content values to obtain the corresponding concentrations of $VK_1(H_2O)_x^{-\bullet}$ (Table 1).

The data in Table 1 indicate that there is a substantial amount of $VK_1(H_2O)_x^{-\bullet}$ present (up to 35%) when electrolysis is carried out under the high-water conditions, which provides an alternative estimate to the quantities of radicals compared to

Table 1. Concentration of $VK_1^{-\bullet}$ in Solutions from EPR Signal Intensity Measurements

n (electrons per molecule)	concentration of $VK_1^{-\bullet}$ in low-water-content solution (mol $L^{-1} \times 10^3$)	concentration of $VK_1(H_2O)_x^{-\bullet}$ in high-water-content solution (mol $L^{-1} \times 10^3$)
0.2	0.20	0.03
0.4	0.40	0.10
0.6	0.60	0.21
0.8	0.80	0.26
1.0	1.00	0.33

dx.doi.org/10.1021/jp4003966 | J. Phys. Chem. B 2013, 117, 2396−2402

calculations based on comproportionation equilibrium constants (K_c) measured using electrochemical methods. The K_c reaction is given in eq 9 (excluding hydrogen-bonding interactions with water) whose value can be estimated electrochemically using eq 10 (provided $E^0_{f(1)}$ and $E^0_{f(2)}$ are known). Under low-water conditions, the separation between the first and second reduction potentials is so great that the forward reaction in eq 5 is strongly favored. This means that under low-water conditions $VK_1^{-\bullet}$ will exist in its monoradical form and will not be able to be converted into VK_1^{2-} until all of the VK_1 in solution is first converted into $VK_1^{-\bullet}$.

$$K_c = \frac{[VK_1^{-\bullet}]^2}{[VK_1^{2-}][VK_1]} \tag{9}$$

$$K_c = \exp\left[\frac{(E^0_{f(1)} - E^0_{f(2)})F}{RT}\right] \tag{10}$$

One problem in calculating K_c values of quinones in nonaqueous solvents is that they are highly dependent on the water content of the solvent, since even small changes to the trace water can shift $E^0_{f(2)}$ and therefore alter K_c. A further complication in calculating K_c values in both aqueous and nonaqueous solvents is that it is not always possible to know the exact form that the compound exists in, since the quinone (and especially its reduced forms) undergoes some degree of hydrogen bonding with water.[5,8]

A more accurate mechanism for the reduction of quinones in the presence of water is given in Scheme 2, where electron

Scheme 2. Electron Transfer and Hydrogen-Bonding Interactions during the Reduction of Quinones in the Absence of Acid

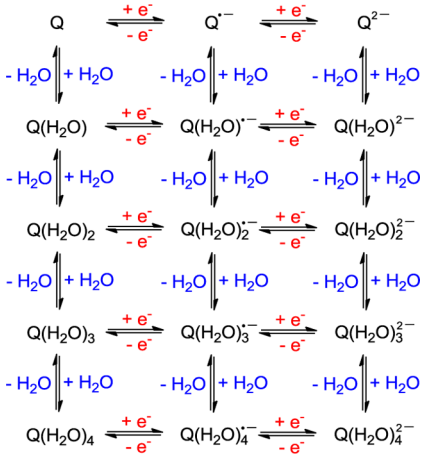

transfer reactions are drawn horizontally and homogeneous reactions with water are drawn vertically.[10] More interactions with water can be included in Scheme 2, since the maximum is not limited to four.[6] Each electron transfer reaction in Scheme 2 has an associated reduction potential and each homogeneous reaction with water has an associated equilibrium constant. Thus, the species given in eq 9 are likely to exist in equilibrium with other hydrogen-bonded species, although the exact number of water molecules involved in the reactions and corresponding equilibrium constants are not known. Furthermore, $E^0_{f(1)}$ and $E^0_{f(2)}$ in eq 10 comprise a number of electrode potentials, as shown in Scheme 2, depending on the degree of hydrogen bonding with water. Therefore, because of the large number of species that are in equilibrium and whose individual concentrations are unknown, it is difficult to derive an equilibrium expression that allows the direct calculation of K_c from the signal intensity measurements given in Table 1.

3.3. ATR-FTIR Spectroscopy. FTIR experiments were performed by electrolyzing the sample in a controlled potential electrolysis cell with an ATR diamond composite sensor positioned in the working electrode compartment. The ATR-FTIR sensor has a usable wavelength range between 1900 and 650 cm^{-1}. The technique is significantly less sensitive than EPR spectroscopy, so experiments needed to be conducted with a relatively high VK_1 concentration of 0.02 M. The solvent/electrolyte (CH_3CN/Bu_4NPF_6) does not absorb strongly within the wavelength range used (1900−900 cm^{-1}), although H_2O does absorb very strongly between 1700 and 1600 cm^{-1}. Therefore, these experiments were conducted using the low-water-content CH_3CN (≤50 mM H_2O) to avoid interferences in the carbonyl stretching region.

The electrolysis experiments were conducted by first applying a potential that was sufficiently negative to reduce VK_1 to $VK_1^{-\bullet}$ but not high enough to further reduce $VK_1^{-\bullet}$ to VK_1^{2-}. After the exhaustive generation of $VK_1^{-\bullet}$, a more negative potential was applied to reduce $VK_1^{-\bullet}$ to VK_1^{2-}. After recording ATR-FTIR spectra at each stage, VK_1^{2-} was oxidized back to the starting material by applying an oxidizing potential (0 V vs Ag wire). With the low-water concentrations used for these measurements, $VK_1^{-\bullet}$ will exist mainly in its non-hydrogen-bonded form, while VK_1^{2-} will exist as $VK_1(H_2O)_y^{2-}$.[5,6]

Figure 4 shows the FTIR spectra of VK_1 and its reduced forms obtained during the electrolysis in CH_3CN. The FTIR

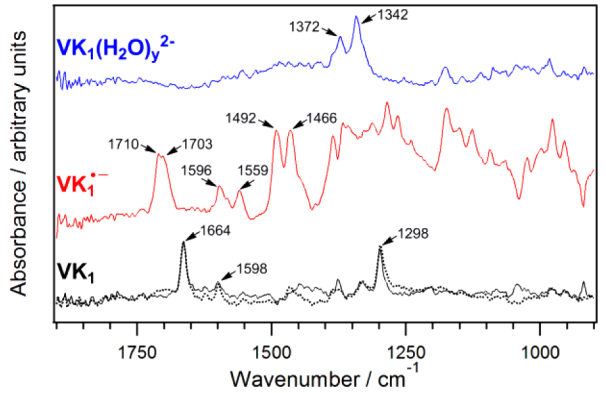

Figure 4. *In situ* ATR-FTIR spectra recorded during the electrolysis of 20 mM VK_1 (black line) in CH_3CN containing 0.2 M Bu_4NPF_6 at 22 ± 2 °C with 0.05 M H_2O. $VK_1^{-\bullet}$ (red line) and $VK_1(H_2O)_y^{2-}$ (blue line) were prepared by applying a reducing potential 0.2 V more negative than $E^0_{f(1)}$ and $E^0_{f(2)}$, respectively. The dotted black line is the spectrum of VK_1 that was regenerated from $VK_1(H_2O)_y^{2-}$ by applying an oxidative potential.

spectrum of the neutral starting material, VK_1, shows characteristic bands between 1700 and 1200 cm^{-1}. The more intense bands arise from C═O stretching vibrations as well as symmetric and asymmetrical C═C ring stretching vibrations. These bands are typically located between 1692 and 1560 cm^{-1} based on theoretical calculations,[25] experimental data,[26] and results from using isotopically labeled 2,3-dimethoxy-5-methyl-6-decaisoprenyl-1,4-benzoquinone.[27] The sharp and intense

dx.doi.org/10.1021/jp4003966 | J. Phys. Chem. B 2013, 117, 2396−2402

band at 1664 cm^{-1} is assigned to the C═O stretch and the band at 1598 cm^{-1} to the symmetric C═C ring stretching vibration in VK_1. The assignment of the C═O and C═C stretching bands to single IR bands is facilitated since both of these modes are allowed to be closely approximated as group vibrations.[25,28] It is mostly the electronic effects of the substituent on the quinone ring in VK_1 that will determine the exact positions of the C═O and ring stretching C═C bands, and only to a small extent by interactions with other molecules, e.g., hydrogen bonding to water found in the solvent. Since the quinone structure in VK_1 is asymmetrically substituted, two C═O stretching bands are expected. However, it is often difficult to clearly differentiate the two individual bands due to overlapping absorbances. The assignment of bands in the remaining region between 1500 and 1200 cm^{-1} is less certain and will be neglected here, since it does not contain valuable information to aid in the understanding of the IR spectra.

Upon the first reduction at an applied potential of −0.9 V vs Ag wire (0.5 M Bu_4NPF_6 in CH_3CN) to generate $VK_1^{-\bullet}$ (Figure 4, red line), the color of the solution changed from yellow to dark green, and the intense band at 1664 cm^{-1} in the spectrum disappeared. Two new intense and partly overlapping absorbances appeared at 1710 and 1703 cm^{-1}, which are likely to originate from the C═O stretching vibrations. Two new intense bands were also observed at 1596 and 1559 cm^{-1}, which are possibly associated with the symmetric and asymmetric C═C ring stretching modes. Comparing the positions of the C═O bands belonging to VK_1 and $VK_1^{-\bullet}$, it is apparent that the C═O absorbance in the radical anion is located at a higher wavenumber (hence a stronger bond) than the C═O band in VK_1. The stronger C═O bond can be attributed to the increased electron density being distributed in the aromatic ring. This observation is consistent with the CV results obtained in this and previous studies which have shown that the potential of the first reduction peak does not change much with varying water concentration, suggesting that the electron densities at the oxygen atoms in $VK_1^{-\bullet}$ are not very different from neutral VK_1.[5,6] The presence of the C═C ring stretching bands indicates that the radical maintains its quinone-like structure, as shown in Scheme 1.

When a potential of −1.6 V vs Ag wire (0.5 M Bu_4NPF_6 in CH_3CN) was applied in the electrolysis cell, the second one-electron reduction process occurred, forming the dianion with the solution changing from a dark green to a dark maroon color. From the ATR-FTIR spectrum of $VK_1(H_2O)_y^{2-}$ shown in Figure 4 (blue line), it can be seen that the two C═O bands at 1710 and 1703 cm^{-1} have disappeared as well as the C═C ring stretching modes. The only strong bands observed in the FTIR spectrum of the dianion (between 1900 and 900 cm^{-1}) occurred at 1372 and 1342 cm^{-1}, and these are tentatively assigned to the two C−O single bond stretches present in the dianion structure. The lack of absorbances in the FTIR spectrum of the dianion between 1800 and 1500 cm^{-1} suggests that the compound is largely aromatic in character, containing weaker C−O bonds with higher electron density at the oxygen atoms (as drawn in Scheme 1). Such higher electron density is consistent with CV data, which indicate that the dianions undergo stronger hydrogen-bonding interactions with water molecules.

When $VK_1(H_2O)_y^{2-}$ was electrochemically oxidized by applying 0 V to the electrode surface, the color of the solution changed from dark maroon to yellow, indicating that VK_1 was being completely regenerated from its reduced forms in the solution. Furthermore, the FTIR spectrum of the reoxidized solution only displayed the characteristic bands of the starting material at 1664 and 1598 cm^{-1} (Figure 4, dotted black line), thereby reaffirming that the reduced states were stable on the time scale of the experiment (approximately 60 min).

Upon the completion of the electrolysis, KF titrations were carried out separately on the solutions contained in the cathodic and anodic compartments. It was found that, although the volume of the anodic compartment solution was 4 times the volume of the solution in the cathodic compartment; the water content in the cathodic compartment solution where the reduced species were generated was approximately twice the water content found in the anodic compartment solution. Hence, it is possible that the water molecules from the anodic compartment were transferred into the cathodic compartment during the course of the second reduction process, due to the ability of the highly charged oxygen atoms in VK_1^{2-} to undergo strong hydrogen bonding with water. An equilibrium exists between the rate at which the water enters and exits the cathodic compartment. KF titrations suggest that the rate of water leaving the cathodic compartment after reoxidation is much slower than the rate of uptake during the second reduction step. Consequently, the water content in the cathodic compartment is greater than that found in the anodic counterpart.

4. CONCLUSION

The reduction of VK_1 in organic solvents containing large amounts of water occurs in a two-electron process to initially form the dianion, which subsequently undergoes a comproportionation reaction with the starting material to form the semiquinone anion radical. Quantitative EPR spectroscopic experiments indicate that, when 1×10^{-3} M solutions of VK_1 were reduced in acetonitrile containing 7.22 M water, $VK_1(H_2O)_x^{-\bullet}$ was generated in up to 35% yield based on the charge passed for a one-electron reduction. The comproportionation reaction is itself very complicated because there are likely to exist a number of different forms of $VK_1^{-\bullet}$ and VK_1^{2-} present in equilibrium and undergoing hydrogen bonding with water (e.g., $[VK_1(H_2O)_x^{-\bullet}]$ and $[VK_1(H_2O)_y^{2-}]$). *In situ* ATR-FTIR spectra were obtained of $VK_1^{-\bullet}$ and $VK_1(H_2O)_y^{2-}$ by sequential one- and two-electron reductive electrolysis in low-water-content acetonitrile. The FTIR spectra supported the assignment of the quinone form of $VK_1^{-\bullet}$ containing C═O groups, and the largely aromatic form of $VK_1(H_2O)_y^{2-}$ containing C—O groups with strongly electronegative oxygen atoms.

■ ASSOCIATED CONTENT

Ⓢ Supporting Information

Intensities of the integrated EPR signals at different electrolysis levels and times after the completion of the electrolysis, for experiments in low-water and high-water conditions. This material is available free of charge via the Internet at http://pubs.acs.org.

■ AUTHOR INFORMATION

Corresponding Author

*E-mail: webster@ntu.edu.sg.

Notes

The authors declare no competing financial interest.

dx.doi.org/10.1021/jp4003966 | J. Phys. Chem. B 2013, 117, 2396−2402

■ ACKNOWLEDGMENTS

This work was supported by an A*Star SERC Public Sector Funding (PSF) Grant (112 120 2006).

■ REFERENCES

(1) Garber, A. K.; Binkley, N. C.; Krueger, D. C.; Suttie, J. W. *J. Nutr.* **1999**, *129*, 1201−1203.
(2) Miggiano, G. A.; Robilotta, L. *Clin. Ter.* **2005**, *156*, 41−46.
(3) Voet, D. *Biochemistry*; John Wiley & Sons: New York, 1990; p 1223.
(4) Josic, D.; Hoffer, L.; Buchacher, A. *J. Chromatogr., B* **2003**, *790*, 183−197.
(5) Hui, Y.; Chng, E. L. K.; Chng, C. Y. L.; Poh, H. Y.; Webster, R. D. *J. Am. Chem. Soc.* **2009**, *131*, 1523−1534.
(6) Hui, Y.; Chng, E. L. K.; Chua, L. P.-L.; Liu, W. Z.; Webster, R. D. *Anal. Chem.* **2010**, *82*, 1928−1934.
(7) *Organic Electrochemistry*, 3rd ed.; Lund, H., Baizer, M. M., Eds.; Marcel Dekker: New York, 1991.
(8) Gupta, N.; Linschitz, H. *J. Am. Chem. Soc.* **1997**, *119*, 6384−6391.
(9) Quan, M.; Sanchez, D.; Wasylkiw, M. F.; Smith, D. K. *J. Am. Chem. Soc.* **2007**, *129*, 12847−12856.
(10) Webster, R. D. *Chem. Rec.* **2012**, *12*, 188−200.
(11) Yang, J. E.; Yoon, J.-H.; Won, M.-S.; Shim, Y.-B. *Bull. Korean Chem. Soc.* **2010**, *31*, 3133−3138.
(12) Belding, S. R.; Limon-Petersen, J. G.; Dickinson, E. J. F.; Compton, R. G. *Angew. Chem., Int. Ed.* **2010**, *49*, 9242−9245.
(13) Wang, Y.; Rogers, E. I.; Belding, S. R.; Compton, R. G. *J. Electroanal. Chem.* **2010**, *648*, 134−142.
(14) Tang, Y.; Wu, Y.; Wang, Z. *J. Electrochem. Soc.* **2001**, *148*, E133−E138.
(15) Jin, B.; Huang, J.; Zhao, A.; Zhang, S.; Tian, Y.; Yang, J. *J. Electroanal. Chem.* **2010**, *650*, 116−126.
(16) Roginsky, V. A.; Pisarenko, L. M.; Bors, W.; Michel, C. *J. Chem. Soc., Perkin Trans. 2* **1999**, 871−876.
(17) Webster, R. D. *J. Chem. Soc., Perkin Trans. 2* **2002**, 1882−1888.
(18) Hui, Y.; Webster, R. D. *Anal. Chem.* **2011**, *83*, 976−981.
(19) Fritsch, J. M.; Tatwawadi, S. V.; Adams, R. N. *J. Phys. Chem.* **1967**, *71*, 338−342.
(20) Das, M. R.; Connor, H. D.; Leniart, D. S.; Freed, J. H. *J. Am. Chem. Soc.* **1970**, *92*, 2258−2268.
(21) Joela, H.; Lehtovuori, P. *Phys. Chem. Chem. Phys.* **1999**, *1*, 4003−4010.
(22) Valko, M.; Morris, H.; Mazúr, M.; Rapta, P.; Bilton, R. F. *Biochim. Biophys. Acta* **2001**, *1527*, 161−166.
(23) Epel, B.; Niklas, J.; Sinnecker, S.; Zimmermann, H.; Lubitz, W. *J. Phys. Chem. B* **2006**, *110*, 11549−11560.
(24) Sinnecker, S.; Reijerse, E.; Neese, F.; Lubitz, W. *J. Am. Chem. Soc.* **2004**, *126*, 3280−3290.
(25) Girlando, A.; Pecile, C. *J. Mol. Spectrosc.* **1979**, *77*, 374−384.
(26) Flaig, W.; Salfeld, J. C. *Ann. Chem.* **1959**, *626*, 215−224.
(27) Bauscher, M.; Mantele, W. *J. Phys. Chem.* **1992**, *96*, 11101−11108.
(28) Colthup, N. B.; Daly, L. H.; Wiberley, S. E. *Introduction to Infrared and Raman Spectroscopy*, 3rd ed.; Academic Press: New York, 1990.